

## Supporting Information

### **Building Additional Passageways in Polyamide Membranes with Hydrostable Metal Organic Frameworks to Recycle and Remove Organic Solutes from Various Solvents**

Xiquan Cheng,<sup>a,b,c</sup> Xu Jiang,<sup>a</sup> Yanqiu Zhang<sup>a</sup> Cher Hon Lau,<sup>\*,b,d</sup> Zongli Xie,<sup>\*,b</sup> Derrick Ng,<sup>b</sup> Stefan J. D. Smith,<sup>b</sup> Matthew R. Hill,<sup>b,e</sup> and Lu Shao<sup>\*a</sup>

#### **Affiliations:**

<sup>a</sup> MIIT Key Laboratory of Critical Materials Technology for New Energy Conversion and Storage, State Key Laboratory of Urban Water Resource and Environment (SKLUWRE), School of Chemistry and Chemical Engineering, Harbin Institute of Technology, Harbin 150001, P.R. China

<sup>b</sup> CSIRO Manufacturing, Private Bag 10, Clayton South VIC 3169, Australia

<sup>c</sup> School of Marine Science and Technology, Sino-Europe Membrane Technology Research Institute, Harbin Institute of Technology, Weihai 264209, P.R. China

<sup>d</sup> School of Engineering, The University of Edinburgh, The King's Buildings, Mayfield Road, EH9 3JL

<sup>e</sup> Department of Chemical Engineering, Monash University, Clayton VIC 3800, Australia

\*Correspondence to: [shaolu@hit.edu.cn](mailto:shaolu@hit.edu.cn), [zongli.Xie@csiro.au](mailto:zongli.Xie@csiro.au), [cherhon.lau@ed.ac.uk](mailto:cherhon.lau@ed.ac.uk)

## Table of Contents

S1. XRD characterization of the MOFs.....	3
S2. Preparation of PA/UiO-66 composite materials and membranes.....	3
S3. Viscosity of PEI/UiO-66 solution .....	4
S4. Fourier transform infrared spectroscopy (FT-IR) of PA/UiO-66 composite materials .....	4
S5. Element analysis of PA/UiO-66 composite materials .....	5
S6. Differential scanning calorimeter (DSC) of polyamide/UiO-66 composite.....	6
S7. Contact angle measurements .....	6
S8. Nanofiltration experiments .....	7
S9. References.....	9

## S1. XRD characterization of the MOFs

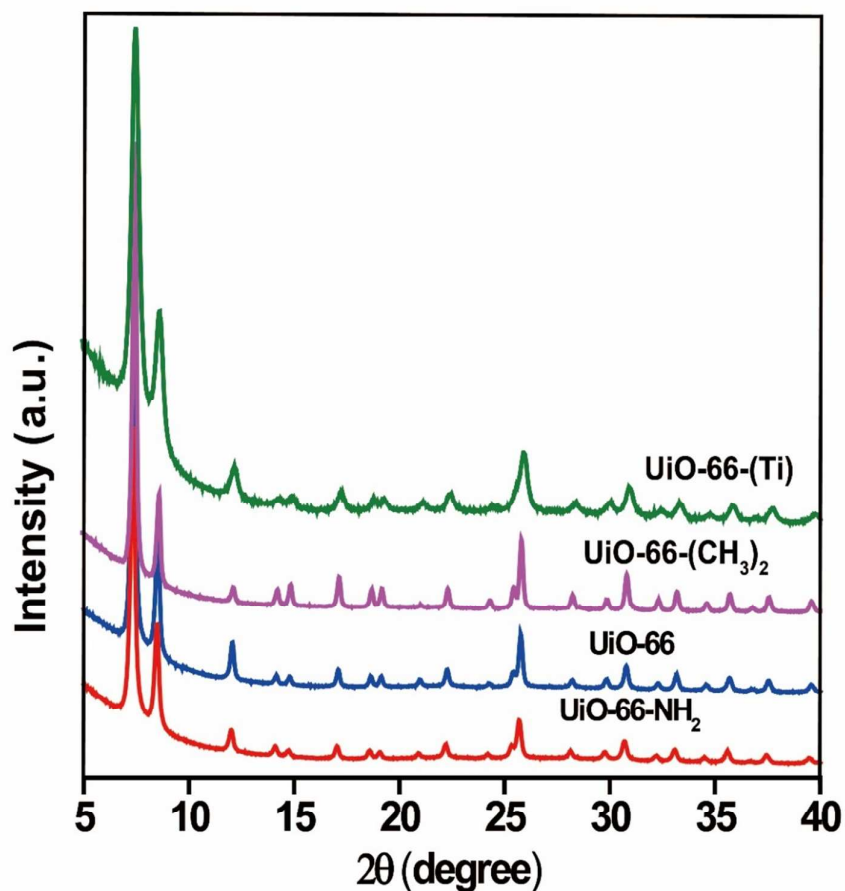


Figure S1. XRD patterns of UiO type MOFs

## S2. Preparation of PA/UiO-66 composite materials and membranes

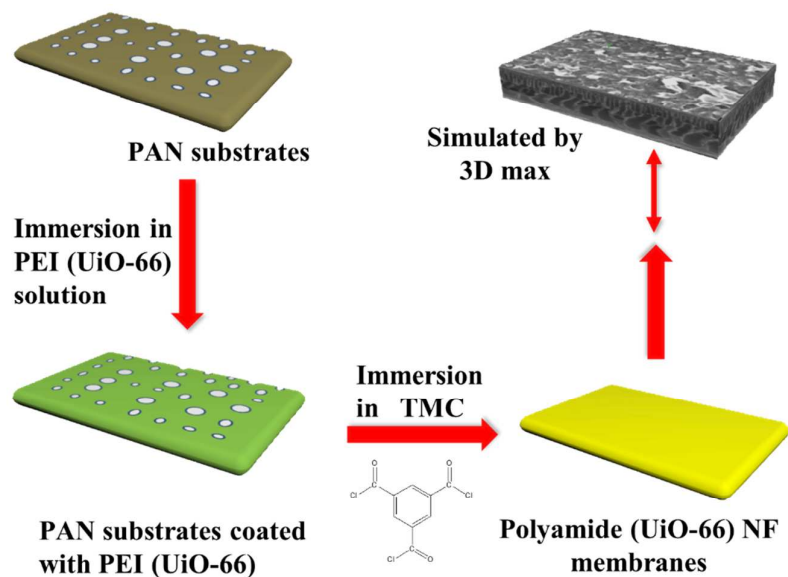
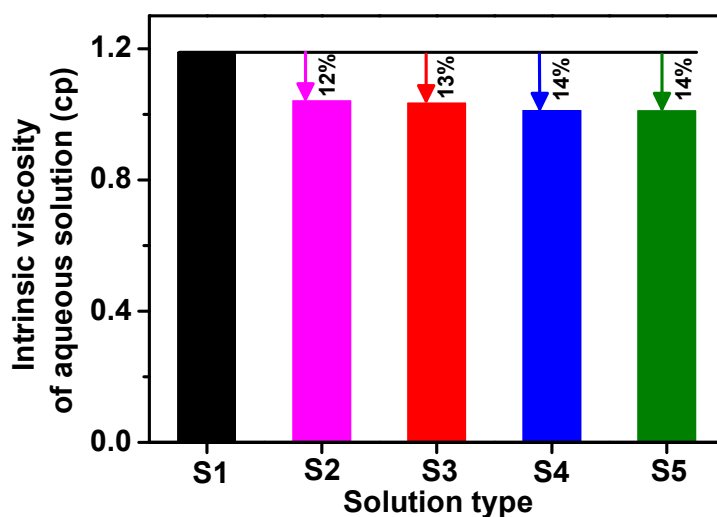


Figure S2. The process of fabrication of polyamide based composite membranes by interfacial polymerization

### S3. Viscosity of PEI/UiO-66 solution

This elucidated the interactions between PEI chains and the UiO-66 additives. **Figure S3** shows that after the addition of 0.2 g UiO-66 to 2 wt.% PEI solution, the viscosity of the mixture declined by 12~14%. This can be attributed to UiO-66 limiting the entanglement of PEI chain. This phenomenon might be due to some non-bonding interaction between the side chain of the branched PEI and the UiO-66. To further confirm this results, the zeta potential of the UiO-66 and UiO-66-NH<sub>2</sub> were characterized by a nanoparticle analyzer (Zetasizer Nano, Malvern Instruments Ltd.). The zeta potential of the UiO-66 and UiO-66-NH<sub>2</sub> were about 23.7 and 18.5 mV, respectively, indicating the UiO-66 based nanoparticles demonstrate positive charged. Thus, the non-bonding interaction contributes all of the viscosity decline of the solutions after adding the UiO-66 nanoparticles in the solutions. Similar phenomenon was also found in other work.<sup>1,2</sup>



**Figure S3.** The viscosity of the solutions. S1 contains only 2.0 wt.% of PEI solution, S2~S5 solutions contain 2.0 wt.% PEI with 0.2 wt.% of UiO-66-(CH<sub>3</sub>)<sub>2</sub> (S2), UiO-66-NH<sub>2</sub> (S3), UiO-66 (S4) and UiO-66-(Ti) (S5).

### S4. Fourier transform infrared spectroscopy (FT-IR) of PA/UiO-66 composite materials

The ATR-FTIR spectrum of reactants TMC and branched PEI are shown in **Figure S5**. In the spectrum of TMC, the peak at 1741 cm<sup>-1</sup> belongs to the C=O in the acyl chloride group.<sup>2</sup> For the spectrum of PEI, the peak at 3277 cm<sup>-1</sup> is the -NH stretching vibration peak, and the peak ranging from 2882 to 2887 cm<sup>-1</sup> belongs to the -CH stretching vibration peak. The peak at 1584 cm<sup>-1</sup>, 1443 cm<sup>-1</sup> and 1347<sup>-1</sup>, are attributed to N-H in-plane bending vibration peak, C-H in-plane vibration peak, C-N stretching vibration peak, respectively.<sup>3-4</sup> After interfacial polymerization, the absorption of -C=O of acyl chloride shifted to 1614 cm<sup>-1</sup>. This is due to the transformation of acyl chloride group to C=O-NH. Furthermore, the peak at 1547 cm<sup>-1</sup> belongs to C-N in C=O-NH; indicating the formation of -C=O-NH group as well.<sup>5</sup> After incorporation of UiO-66, the peaks around 2880 cm<sup>-1</sup> weakened and new peaks around 1000 cm<sup>-1</sup> occurred; indicating that some interaction between the UiO-66 and polyamide.

This kind interaction may derive from non-bonding interaction between the side chain of the branched PEI and the UiO-66.

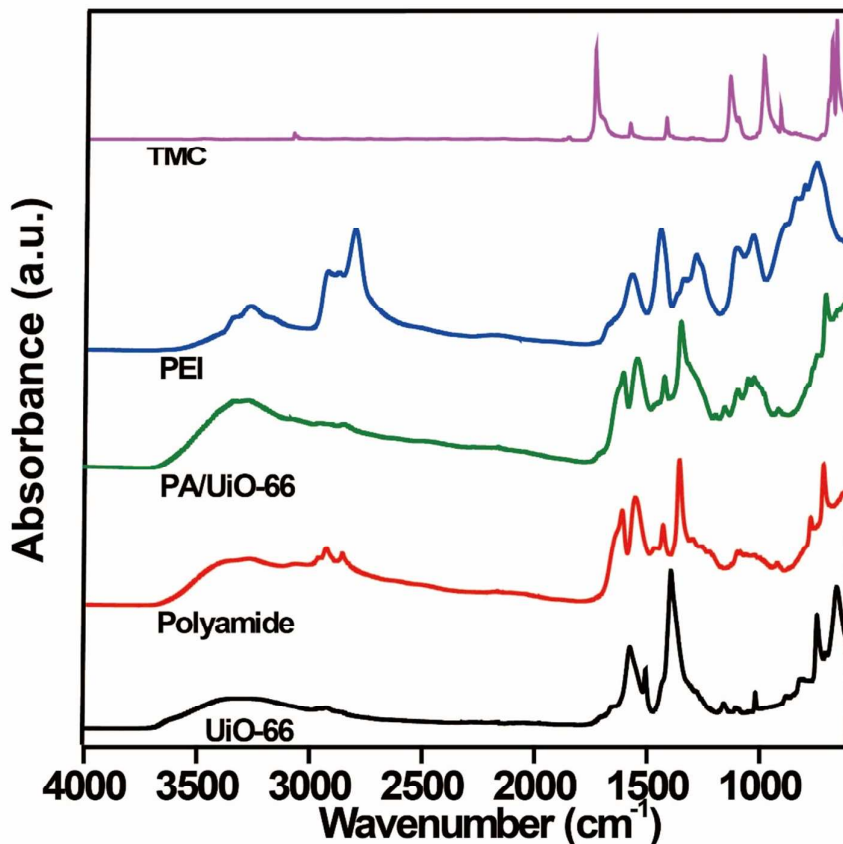


**Figure S4.** The FT-IR of monomers, UiO-66 additives, and polyamide or polyamide/UiO-66 composite materials.

### S5. Element analysis of PA/UiO-66 composite materials

After incorporating different type of UiO-66, the Zr element was detected in the polyamide/UiO-66 composite materials, indicating that the UiO-66 was successfully loaded in the polyamide based composite materials.

**Table S1.** The element content of polyamide based composite materials

Samples	Element content (At. %)				
	C	N	O	Zr	Ti
PA	77.5	12.8	9.7	--	--
PA/UiO-66	75.9	11.5	11.8	0.8	--
PA/UiO-66-NH <sub>2</sub>	75.2	13.1	11.1	0.6	--
PA/UiO-66-(CH <sub>3</sub> ) <sub>2</sub>	76.4	11.4	11.5	0.7	--
PA/UiO-66 (Ti)	75.4	11.7	12.0	0.5	0.4

## S6. Differential scanning calorimeter (DSC) of polyamide/UiO-66 composite

T<sub>g</sub> values were taken from the second heating cycle. The DSC curves of polyamide based composite materials was depicted in **Figure S6**. The T<sub>g</sub> of polyamide prepared by interfacial polymerization of PEI and TMC is about 45.9 °C. After incorporation of UiO-66, the T<sub>g</sub> increased slightly to 47.5 °C and 48.3 °C, indicating good compatibility of UiO-66 and polyamide.

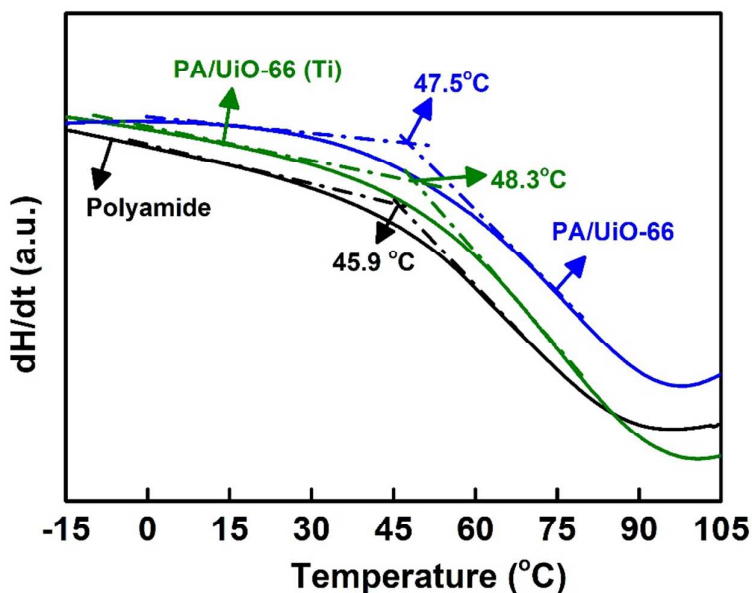


**Figure S5.** The DSC curves of the polyamide/UiO-66 composite materials

## S7. Contact angle measurements

With water contact angle of 55°, the surface of pristine polyamide membrane is hydrophilic. In the polyamide structures fabricated by PEI, some amino groups might not react with TMC due to steric effects. Therefore, the surfaces of polyamide are more hydrophilic than PAN substrates. After incorporation of UiO-66, the water contact angle of the membranes increased slightly. UiO-66 MOFs are known to be hydrophobic, hence reducing the hydrophilicity of resultant PA/MOF composites.

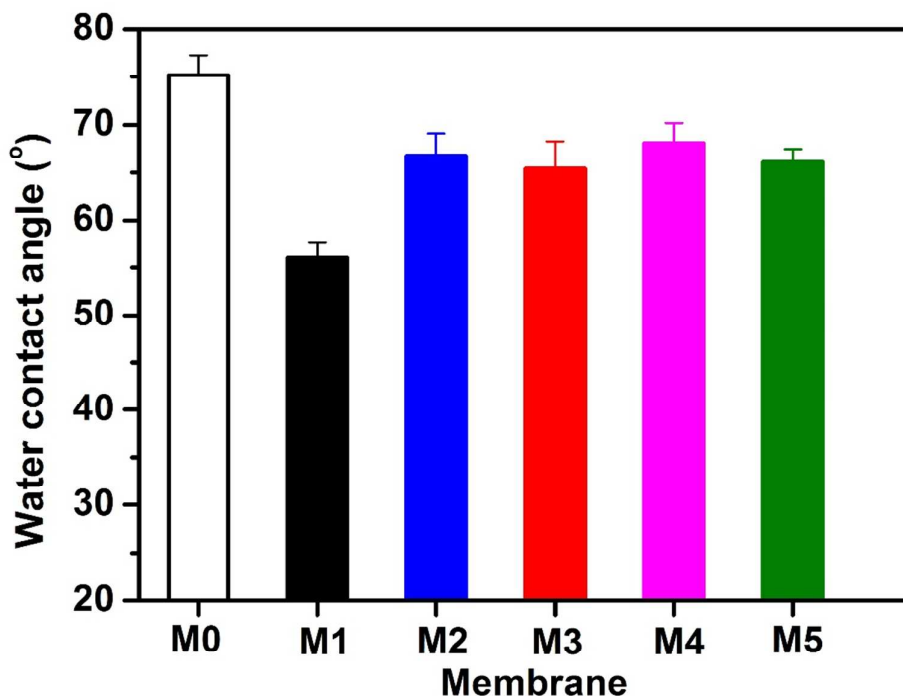


**Figure S6.** Contact angles of fabricated membranes: M0= PAN substrates, M1=polyamide membrane, M2=PA/UiO-66 membrane; M3=PA/UiO-66-NH<sub>2</sub> membrane; M4=PA/UiO-66-(CH<sub>3</sub>)<sub>2</sub> membranes, M5=polyamide/UiO-66-(Ti) membrane

## S8. Nanofiltration experiments

Since the permeance of our membranes is high, the concentration polarization phenomenon might be serious. The absorbance of the concentrate of RB solution was measured by UV-Vis to evaluate the concentration, which was shown in **Figure S8**. After the filtration, the concentration of the feed solution increased above 200%. Considering the concentration of the solutions near the membranes is much higher than that of bulk solution during the measurement, the CP affect the mass transfer of RB solution indeed. In this circumstances, our membranes still showed high rejections to organic solutes, confirming the excellent performance of our membranes. To simulate the separation performance of PA/UiO-66 membranes under concentration polarization, we also measured the RB rejection and permeance of RB solution varying with the feed concentration. With the increment of the RB concentration, both the permeances and the rejection of our membranes slightly declined. Interestingly, our membranes demonstrate RB rejection as high as 99.5 % even under high concentration (1000 ppm), confirming that our membranes could demonstrate high separation performance at high concentration polarization level (**Figure 10**).

We also compared the separation performances of our membranes in water/organic solvents with those reported in literature (**Figure 5**).<sup>6-17</sup> From the results, the permeances of the PA/UiO-66 membranes are much higher than other kinds of nanofiltration membranes with comparable or even higher rejection performances when separating the RB from water. For separating Rose Bengal in methanol, the rejection of the PA/UiO-66 is about 97.5%, which is comparable with commercial membranes (**SW30HR** and **DuraMem DM150**). Interestingly, the permeance of the PA/UiO-66

membranes is about 3 times higher than that of commercial OSN membranes. For the thin polyamide membranes building nanochannels by etching the  $\text{Cd}(\text{OH})_2$  nanostrands, the MeOH permeance is higher than that of our membranes. However, it is hard to get defect-free membranes in large scale through this method and the etching of  $\text{Cd}(\text{OH})_2$  will generate  $\text{Cd}^{2+}$  which is harmful for water. Meanwhile, the membranes demonstrate high 97.6% rejections of azithromycin with high flux as well (discussed in manuscript), a typical of antibiotics. Taken together, the PA/UiO-66 membranes show strong promise in separating organic contaminants including dyes and antibiotics from both water and organic solvents.

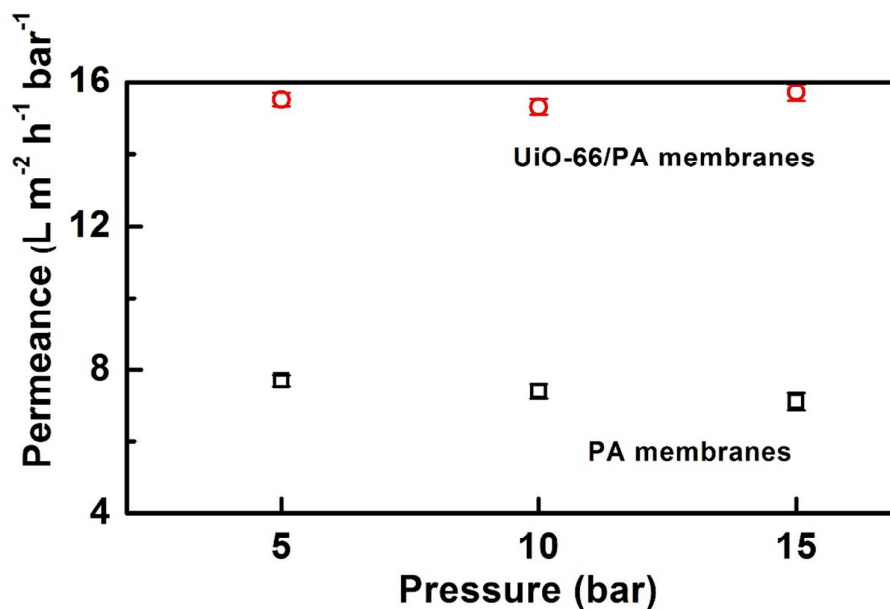


**Figure S7.** The effects of the pressure on the water permeances of the composite nanofiltration membranes

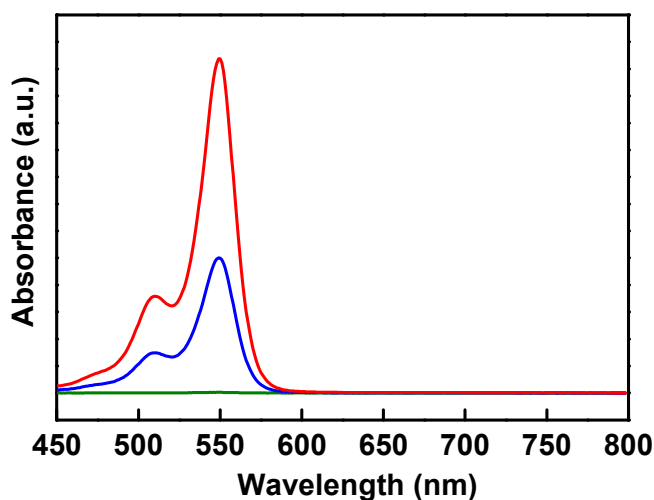


**Figure S8.** The UV-Vis spectra of the dye solution; blue: feed solution; green: permeate solution; red: concentrate solution

## S9. References

1. Lau, C. H.; Konstas, K.; Thornton, A. W.; Liu, A. C.; Mudie, S.; Kennedy, D. F.; Howard, S. C.; Hill, A. J.; Hill, M. R., Gas-Separation Membranes Loaded with Porous Aromatic Frameworks that Improve with Age, *Angew. Chem. Int. Edit.* **2015**, *54*, 2669-2673.
2. Lau, C. H.; Mulet, X.; Konstas, K.; Doherty, C. M.; Sani, M. A.; Separovic, F.; Hill, M. R.; Wood, C. D., Hypercrosslinked Additives for Ageless Gas-Separation Membranes, *Angew. Chem. Int. Edit.* **2016**, *55*, 1998-2001.
3. Liu, M.; Zheng, Y.; Shuai, S.; Zhou, Q.; Yu, S.; Gao, C, Thin-Film Composite Membrane Formed by Interfacial Polymerization of Polyvinylamine (PVAm) and Trimesoyl Chloride (TMC) for Nanofiltration, *Desalination*, **2012**, *288*, 98-107.
4. Liu, M.; Ji, J.; Zhang, X.; Zhang, X.; Yang, B.; Deng, F.; Li, Z.; Wang, K.; Yang, Y.; Wei, Y, Self-Polymerization of Dopamine and Polyethyleneimine: Novel Fluorescent Organic Nanoprobes for Biological Imaging Applications, *J. Mater. Chem. B* **2015**, *3*, 3476-3482.
5. Rao, P. S.; Smitha, B.; Sridhar, S.; Krishnaiah, A., Preparation and Performance of Poly (vinyl alcohol)/polyethyleneimine Blend Membranes for The Dehydration of 1, 4-dioxane by Pervaporation: Comparison with Glutaraldehyde Cross-linked Membranes, *Sep. Purif. Technol.* **2006**, *48*, 244-254.
6. Wu, D.; Huang, Y.; Yu, S.; Lawless, D.; Feng, X., Thin Film Composite Nanofiltration Membranes Assembled Layer-by-layer via Interfacial Polymerization from Polyethylenimine and Trimesoyl Chloride *J. Membr. Sci.* **2014**, *472*, 141-153.
7. Nam, Y. T.; Choi, J.; Kang, K. M.; Kim, D. W.; Jung, H.-T., Enhanced Stability of Laminated Graphene Oxide Membranes for Nanofiltration via Interstitial Amide Bonding. *ACS Appl. Mater. Interfaces* **2016**, *8*, 27376-27382.
8. Mahdavi, H.; Razmi, F.; Shahalazade, T., Polyurethane TFC Nanofiltration Membranes Based on Interfacial Polymerization of Poly (bis-MPA) and MDI on the Polyethersulfone Support. *Sep. Purif. Technol.* **2016**, *162*, 37-44.
9. Liu, L.; Wang, X.; Wang, Y.; Li, L.; Pan, K.; Yang, J.; Cao, B., Preparation and Characterization of Asymmetric Polyarylene Sulfide Sulfone (PASS) Solvent-Resistant Nanofiltration Membranes. *Mater. Lett.* **2014**, *132*, 11-14.
10. Kim, D. W.; Choi, J.; Kim, D.; Jung, H.-T., Enhanced Water Permeation Based on Nanoporous Multilayer Graphene Membranes: the Role of Pore Size and Density. *J. Mater. Chem. A* **2016**, *4*, 17773-17781.
11. Jimenez-Solomon, M. F.; Song, Q.; Jelfs, K. E.; Munoz-Ibanez, M.; Livingston, A. G., Polymer Nanofilms with Enhanced Microporosity by Interfacial Polymerization. *Nat. Mater.* **2016**, *15*, 760-767
12. Echaide-Górriz, C.; Sorribas, S.; Téllez, C.; Coronas, J., MOF Nanoparticles of MIL-68 (Al), MIL-101 (Cr) and ZIF-11 for Thin Film Nanocomposite Organic Solvent Nanofiltration Membranes. *RSC Adv.* **2016**, *6*, 90417-90426.
13. Li, Y.; Wee, L. H.; Volodin, A.; Martens, J. A.; Vankelecom, I. F., Polymer Supported ZIF-8 Membranes Prepared via an Interfacial Synthesis Method. *Chem. Commun.* **2015**, *51*, 918-920.
14. Karan, S.; Jiang, Z.; Livingston, A. G., Sub-10 nm Polyamide Nanofilms with Ultrafast Solvent Transport for Molecular Separation. *Science* **2015**, *348*, 1347-1351
15. Li, X.; Vandezande, P.; Vankelecom, I. F., Polypyrrole Modified Solvent Resistant Nanofiltration Membranes. *J. Membr. Sci.* **2008**, *320*, 143-150.
16. Shao, L.; Cheng, X.; Wang, Z.; Ma, J.; Guo, Z., Tuning the Performance of Polypyrrole-based Solvent-Resistant Composite Nanofiltration Membranes by Optimizing

Polymerization Conditions and Incorporating Graphene Oxide. *J. Membr. Sci.* **2014**, *452*, 82-89.

17. Ahmadiannamini, P.; Li, X.; Goyens, W.; Joseph, N.; Meesschaert, B.; Vankelecom, I. F., Multilayered Polyelectrolyte Complex Based Solvent Resistant Nanofiltration Membranes Prepared from Weak Polyacids. *J. Membr. Sci.* **2012**, *394*, 98-106.
18. Hendrix, K.; Van Eynde, M.; Koeckelberghs, G.; Vankelecom, I. F., Crosslinking of Modified Poly (ether ether ketone) Membranes for Use in Solvent Resistant Nanofiltration. *J. Membr. Sci.* **2013**, *447*, 212-221.